References and Notes

1. J. R. Luyten and J. Swallow, *Deep-Sea Res.* **23**, 1005 (1976).
2. J. R. Luyten, *Equat. Curr. Meas.*, in press.
3. C. C. Eriksen, *Deep Currents and Equatorial Waves*, in press.
4. S. Hayes and H. Milburn, *J. Phys. Oceanogr.*, in press.
5. D. W. Moore and S. G. H. Philander, in *The Sea*, E. D. Goldberg *et al.*, Eds. (Interscience, New York, 1976), vol. 6, pp. 319-362.
6. C. Wunsch, *J. Phys. Oceanogr.* **7**, 497 (1977).
7. M. Cane, unpublished manuscript.
8. S. G. M. Philander and P. C. Pacanowski, *J. Geophys. Res.*, in press.
9. K. Wyrtki, *Science* **181**, 262 (1973).
10. R. Knox, *Deep-Sea Res.* **23**, 211 (1976).
11. M. Greig and P. Cresswell, *Satellite Tracked Buoy Data: Pacific and Indian Oceans* (Commonwealth Scientific and Industrial Research Organization, Cronulla, New South Wales, 1979).
12. J. J. O'Brien and H. E. Hulburt, *Science* **184**, 1075 (1974).
13. P. Crozet, M. Desbois, A. Semery, P. Sitbon, *Cloud Wind Atlas* (Note LMD 97, Centre National de la Recherche Scientifique, Paris, 1979).
14. Supported by Office of Naval Research, Ocean Science and Technology Division, contracts N00014-76-C-0197 and NR 083-400, National Science Foundation, grant ATM78-21491, and Centre National pour l'Exploitation des Oceans contract CNEXO-79/1971. This is contribution 4521 from Woods Hole Oceanographic Institution.

6 February 1980; revised 19 May 1980

Origin of the Warped Heliospheric Current Sheet

Abstract. *The warped heliospheric current sheet for early 1976 is calculated from the observed photospheric magnetic field by a potential field method. Comparisons with measurements of the interplanetary magnetic field polarity for early 1976 obtained at several locations in the heliosphere by Helios 1, Helios 2, Pioneer 11, and at the earth show a rather detailed agreement between the computed current sheet and the observations. It appears that the large-scale structure of the warped heliospheric current sheet is determined by the structure of the photospheric magnetic field and that "ballerina skirt" effects may add small-scale ripples.*

The magnetic field of the sun is extended outward by the solar wind throughout the solar system. The structure of the extended field has been observed only within 16° of latitude of the solar equator, so that its overall form, containing the well-known magnetic sectors near the equatorial plane, has been a matter of conjecture and debate for many years. The Solar Polar Mission, sometime in the next decade, will probably settle the major questions by direct observation in space. This report describes our present view of the extended structure of the solar magnetic field.

The existence of a warped current sheet in the nonpolar regions of the heliosphere is now generally accepted (*1-4*). An artist's impression of an average shape of the current sheet at a time near sunspot minimum (*2*) is shown in Fig. 1. As the current sheet rotates with the sun, the sector structure of the interplanetary magnetic field (IMF) is produced (*5*). At the phase of the sunspot cycle discussed in this report, the large-scale IMF is directed away from the sun northward of the current sheet and is directed toward the sun southward of the sheet. It should be noted that the term "interplanetary sector structure" coined by Wilcox and Ness (*5*) describes the structure in the plane of the ecliptic and does not refer to three-dimensional structures such as the sections of an orange.

There are two points of view regarding the origin of the warped heliospheric current sheet. Svalgaard and Wilcox (*6*) review the computations of the magnetic field at a "source surface," for which the photospheric magnetic field observed by use of the Zeeman effect serves as a boundary condition. Outside the source surface the warped current sheet is assumed to be carried radially outward by the solar wind. In this model, the structure of the current sheet (the location in solar longitude and the extent in solar latitude of the maxima and minima) is a direct consequence of the observed photospheric magnetic field.

Alfven (*4*) [see also (*7*)] has proposed an alternative viewpoint in which the solar origin of the current sheet is a plane similar to the plane in which the skirt of a ballerina originates (the waist). In this model the current sheet waves up and down like the skirt of a spinning ballerina.

It is our purpose in this report to show that the observations of the IMF during the first months of 1976 (that is, near sunspot minimum) at the earth—by Pioneer 11 near a heliospheric latitude of 16°N (*8*) and by Helios 1 and Helios 2 between 0.28 and 1 A.U. within a latitudinal excursion of ±7.23° from the solar equatorial plane (*9*)—are in good agreement with a warped current sheet computed from the observed photospheric magnetic field by the methods reviewed in (*6*). It thus appears that the large-scale structure of the heliospheric current sheet is controlled by the photospheric magnetic field, although small-scale ripples may be added by dynamic solar wind processes (the ballerina effect).

The curved line in Fig. 2 represents the average warped current sheet that separates regions with magnetic field away from the sun (above the line) and toward the sun (below the line), as computed on a source surface at 2.6 solar radii during the interval 20 January through 26 May 1976. The solar wind is assumed to carry the magnetic structure on the source surface radially outward into the heliosphere. In fact, the curved line in Fig. 2 is similar to the bottom panel of figure 4 in (*6*), which was computed as the average of eighteen 27-day solar rotations starting 5 May 1976 and ending 7 August 1977, just after the interval discussed in this report. This similarity is evidence of the long-term stability of the large-scale photospheric and heliospheric magnetic fields.

Such long-term stability would not be expected from the dynamic effects of the ballerina skirt model. Nor would this stability be expected if the predominant warps in the current sheet were caused by coronal holes (*9*), since the lifetime of a coronal hole is typically only several rotations. Because coronal holes appear in the central portion of sectors (*6*), it would be expected that the longitudes of coronal holes would correspond to the

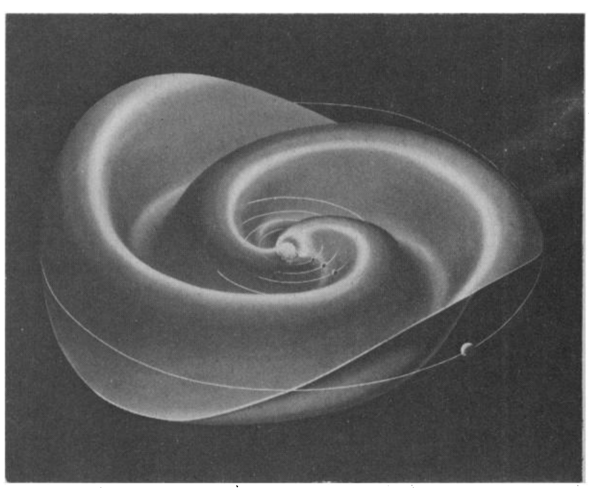

Fig. 1. Artist's impression of the warped heliospheric current sheet. The region above the current sheet has interplanetary magnetic field directed away from the sun and the region below has field directed toward the sun. [Artist: Werner Heil]

0036-8075/80/0801-0603$00.50/0

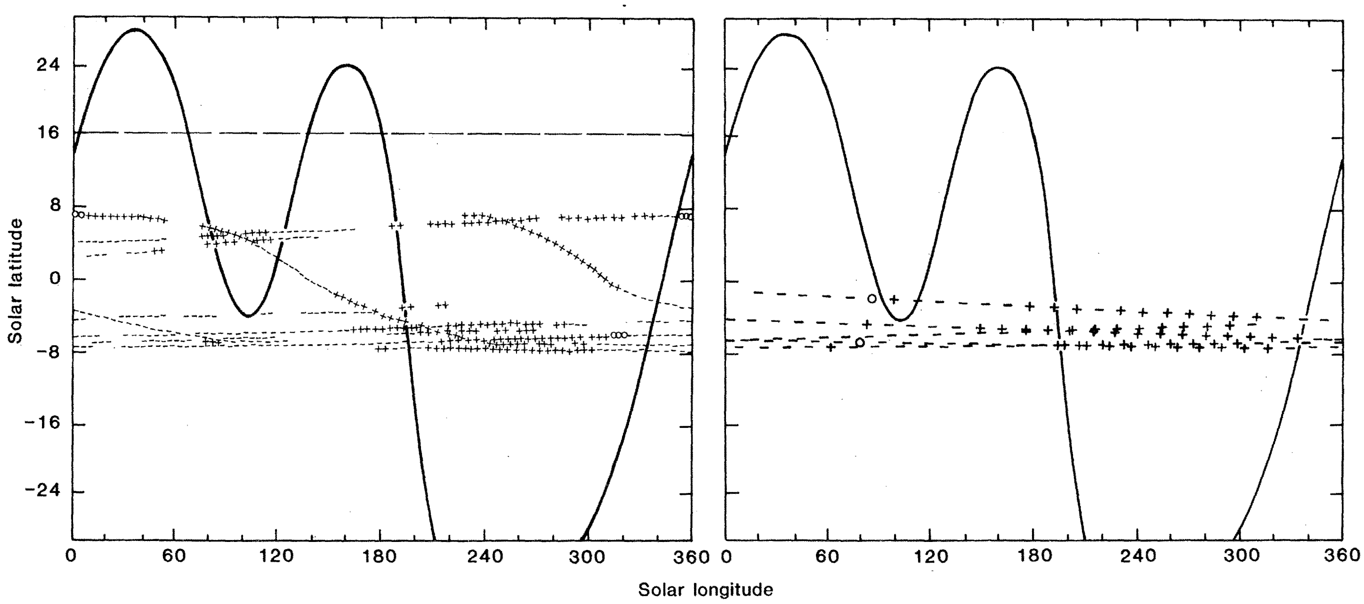

Fig. 2. The curved line represents the calculated average heliospheric current sheet for five rotations from 20 January through 23 May 1976. The dashed line at 16°N latitude represents the approximate heliographic latitude of the Pioneer 11 spacecraft, which was about 4 A.U. from the sun. The plus signs (away from the sun) and minus signs (toward the sun) indicate the IMF polarity measured at Helios 1 and Helios 2 projected back onto the solar corona. The observed IMF polarities agree well with the computed current sheet. Fig. 3. Same as Fig. 2, except that the plus and minus signs represent the inferred IMF polarity at the earth mapped back to the solar corona. The observed polarity changes occur near crossings of the computed current sheet.

longitudes of maximum warp of the heliospheric current sheet.

The dashed horizontal line in Fig. 2 represents the heliographic latitude 16°N, near which Pioneer 11 observed the IMF to be predominantly away from the sun during the interval discussed in this report (*8*). The plus (away) and minus (toward) signs in Fig. 2 represent the IMF polarity as observed by Helios 1 and Helios 2 (*9*) projected onto the solar corona. The computed current sheet in Fig. 2 is similar to the inferred current sheet shown in figure 4b of (*9*).

Figure 2 shows that the Helios spacecraft observations of the polarity of the IMF are in good agreement with the computed location of the current sheet. When the Helios spacecraft were at southern heliographic latitudes a two-sector pattern was observed, whereas when they were at northern latitudes a four-sector pattern was observed, in agreement with Fig. 2.

The curved line in Fig. 2 representing the warped heliospheric current sheet is repeated in Fig. 3, where the plus and minus signs show the inferred IMF polarity at the earth (*10*). A travel time of 4.5 days from the sun to the earth (*11*) is used in mapping this back to the corona. The IMF structure at the earth also shows a two-sector pattern when the earth is near 7°S heliographic latitude, but hints of the four-sector structure are seen as the earth moves northward.

We note that if a travel time of 5.5 days had been used, the data in Fig. 3 would be moved to the right by about 13° of longitude, which would significantly improve the agreement. The same situation exists with regard to the spacecraft data in Fig. 2. This suggests that the simple mapping techniques used in preparing Figs. 2 and 3 may give only an approximation.

Although the large-scale structure of the current sheet persists for many solar rotations, on any particular rotation there may be changes in the current sheet arising from the effects of solar activity and coronal holes (*12*). Nevertheless, the overall agreement in Figs. 2 and 3 between the observed IMF polarities and the structure of the heliospheric current sheet computed from the observed photospheric magnetic field is impressive.

From the considerations discussed in this report we suggest that if Pioneer 11 had been at 16°S heliospheric latitude in the first part of 1976 rather than at 16°N, it would have observed a well-defined sector structure. Also, although Pioneer 11 did observe an IMF polarity that was predominantly away from the sun, we would predict that for intervals of a few days corresponding to Carrington solar longitudes near 35° and 160°, Pioneer 11 may have observed "toward" polarities. We note in figure 2 of Smith *et al.* (*8*) that during the interval of interest the ratio of the number of "away" polarity observations by Pioneer 11 to the total number of observations was about 0.8. The computed current sheet in Fig. 2 of this report corresponds to a ratio of about 0.7.

We suggest that the observations of the IMF polarity by Pioneer 11 and by Helios 1 and Helios 2 support the view that the large-scale structure of the warped heliospheric current sheet can be computed from the observed photospheric magnetic field, with the ballerina effect perhaps adding small-scale ripples. Since coronal holes are effects of conditions pertaining to the large-scale photospheric magnetic configuration (*6*), the influence of coronal holes on the warped current sheet is to a considerable extent already included in the present calculations.

The observations by Pioneer 11 at 16°N heliospheric latitude (*8*) have been misinterpreted as meaning that the heliospheric current sheet is almost parallel to the solar equatorial plane [for example, see (*13*)]. Figure 2 shows that even near the minimum of the 11-year sunspot cycle the current sheet probably reached appreciable south heliospheric latitudes, and the considerations discussed by Svalgaard and Wilcox (*2*) indicate that near the maximum of the sunspot cycle the current sheet reaches heliospheric latitudes of 50° or more (*3*).

J. M. WILCOX
J. T. HOEKSEMA
P. H. SCHERRER

Institute for Plasma Research, Stanford University, Via Crespi, Stanford, California 94305

References and Notes

1. K. H. Schatten, in *Solar Wind*, C. P. Sonett, P. J. Coleman, Jr., J. M. Wilcox, Eds. (National Aeronautics and Space Administration, Washington, D.C., 1972), p. 88; M. Schulz, *Astrophys. Space Sci.* **24**, 371 (1973); E. H. Levy, *Nature (London)* **261**, 394 (1976); M. Schulz, E. N. Frazier, D. F. Boucher, Jr., *Sol. Phys.* **60**, 83 (1978).
2. L. Svalgaard and J. M. Wilcox, *Nature (London)* **262**, 766 (1976).
3. T. Saito, *Sci. Rep. Tohoku Imp. Univ. Ser. 5* **23**, 37 (1975).
4. H. Alfven, *Rev. Geophys. Space Phys.* **15**, 271 (1977).
5. J. M. Wilcox and N. F. Ness, *J. Geophys. Res.* **70**, 5793 (1965).
6. L. Svalgaard and J. M. Wilcox, *Annu. Rev. Astron. Astrophys.* **16**, 429 (1978).
7. E. J. Smith and J. H. Wolfe, *Space Sci. Rev.* **23**, 217 (1979).
8. E. J. Smith, B. T. Tsurutani, R. Rosenberg, *J. Geophys. Res.* **83**, 717 (1978).
9. U. Villante, R. Bruno, F. Marini, L. F. Burlaga, N. F. Ness, *ibid.* **84**, 6641 (1979).
10. L. Svalgaard, *ibid.* **77**, 4027 (1972).
11. J. M. Wilcox, *Space Sci. Rev.* **8**, 258 (1968).
12. R. H. Levine, *Astrophys. J.* **218**, 291 (1977); in *Coronal Holes and High Speed Wind Streams*, J. Zirker, Ed. (Colorado Associated Univ. Press, Boulder, 1977), pp. 103–143.
13. M. A. Livshits, T. E. Valchuk, Y. I. Feldstein, *Nature (London)* **278**, 241 (1979).
14. We thank R. Howard for observations of the photospheric magnetic field obtained at Mount Wilson Observatory. This work was supported in part by the ONR contract N00014-76-C-0207, by NASA grant NGR 05-020-559 and contract NAS5-24420, and by the Atmospheric Sciences Section of the National Science Foundation under grant ATM77-20580.

18 March 1980; revised 5 May 1980

Monozygotic Twin Formation in Mouse Embryos in vitro

Abstract. *Monozygotic twins developed from cultured murine blastocysts at the ratio of approximately 1:100. The locus at which the denuded blastocysts attached to the culture dish was usually a random section of their mural trophoblasts, in which case single egg cylinders developed unilaterally. However, in those few blastocysts attaching with their antipolar mural trophoblasts, the inner cell mass became subdivided into two parts because of restrictions imposed on its growth by the apically situated polar trophoblasts and the plastic substrate. Each subdivision apparently incorporated totipotent cells, resulting in the bilateral formation of two egg cylinders sharing the same ectoplacental cone.*

The cause of monozygotic twinning in mammals, including humans, is not known (*1*). There is strong experimental evidence that in lower vertebrates monozygotic twinning can result from early-stage developmental retardation caused by such factors as lack of oxygen (*2*). In humans, the frequency of congenital malformations in monozygotic twins is nearly twice as high as that in single births, and there is no such increase in dizygotic twins (*3*, *4*). These results indicate that monozygotic twinning is related to some developmental malformation.

In the rat (*5*), rabbit (*6*), and mouse (*7*), it has been demonstrated that single blastomeres of cleaving embryos are totipotent and able to develop into individual animals. However, how and when the monozygotic twins are formed in utero is not known. In vitro, on the other hand, individually cultured mouse embryos are now able to develop far beyond the implantation state (*8*), and thus are amenable to the examination of twin phenomena. The development of monozygotic twins in vitro has been recorded by time-lapse cinematography (*9*).

Development of mouse embryos beyond the implantation stage requires specific macromolecules for growth and differentiation (*10*). Mouse embryos grown in vitro are indistinguishable from those grown in vivo (*11*-*14*), despite the fact that in vitro, blastocysts must attach to and develop on the rigid surface of the plastic culture dish instead of on the flexible uterine endometrium. Still, imposing the mechanical restriction of a culture dish on the developing mouse embryo may cause minor abnormalities. In the present study, we found that cultured blastocysts from random-bred CF 1 mice (6 to 8 weeks old; Charles River) form monozygotic twins at the ratio of nearly 1:100. The cause of these twinnings was traced to the very early development of the embryos at a stage after the attachment of single blastocysts. In this stage, the inner cell mass (ICM) was observed to subdivide and grow as two independent egg cylinders.

The female mice were injected with pregnant mare serum gonadotropin (5 IU; Organon) to stimulate growth of ovarian follicles; human chorionic gonadotropin (5 IU) was injected 48 hours later to stimulate ovulation. They were then placed with males (one pair per cage). The next morning, the females were checked for the presence of a copulatory plug (day 0 of pregnancy). On day 3 of pregnancy, they were killed by cervical dislocation.

All procedures in the preparation, cultivation, and observation of the mouse embryos were conducted at 37°C under either a horizontal or vertical flow hood. The uteri were removed from their mesometria and placed in 100-mm plastic culture dishes. Under a dissecting microscope, each uterine horn was flushed with 1 ml of CMRL 1066 culture medium plus 10 percent heat-inactivated fetal calf serum (FCS) (Grand Island Biological). Blastocysts were sucked into a capillary pipette and pooled in a 35-mm plastic culture dish containing 2 ml of the culture medium. The dish was constantly flushed with a mixture of 5 percent CO_2 and 95 percent air to maintain the *p*H of the medium at 7.4. Ten blastocysts were distributed by capillary pipette into separate culture dishes, each containing 2 ml of culture medium. The cultures were maintained at 38°C in humidified incubators containing 5 percent CO_2 and 95 percent air. The concentration of CO_2 was automatically regulated.

The culture medium was supplemented with 1 m*M* glutamine and 1 m*M* sodium pyruvate; no antibiotics were used at any stage. The concentration of FCS in the medium was increased as the embryos developed. Initially, all blastocysts were cultured in 2 ml of CMRL 1066 plus 10 percent heat-inactivated FCS (day 0 of culture). On day 2 of culture, when the blastocysts had attached to the dishes, the concentration of FCS

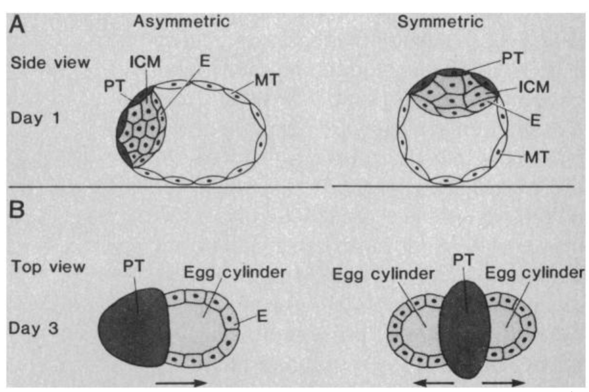

Fig. 1. Schematic drawing of blastocyst attachment (day 1 in culture) and subsequent elongation of the egg cylinder (day 3). (A) Side view of denuded blastocyst attached to the plastic substrate by mural trophoblasts (*MT*) (asymmetric attachment) and by antipolar trophoblasts (symmetric attachment). *E*, Primary endoderm; *ICM*, inner cell mass; *PT*, polar trophoblasts. (B) Top view of development and egg cylinder elongation in asymmetrically attached embryo (left) and symmetrically attached embryo (right). In the asymmetric attachment, while polar trophoblasts proliferate to the left to become the ectoplacental cone, the egg cylinder elongates toward the right. In the symmetric attachment, the polar trophoblasts are positioned above the ICM, and the egg cylinders grow bilaterally away from them.